THERMAL AND THERMO-OXIDATIVE STABILITY OF REPROCESSED POLY (ETHYLENE TEREPHTHALATE)

J.D. Badia, A. Martinez-Felipe, L. Santonja-Blasco, A. Ribes-Greus*

Instituto de Investigación en Tecnología de Materiales.

Universidad Politécnica de Valencia,

Camino de Vera s/n 46071 Valencia, Spain

*To whom correspondence should be addressed.

Corresponding author. Fax: +34963879817

E-mail address: aribes@ter.upv.es

1

THERMAL AND THERMO-OXIDATIVE STABILITY OF REPROCESSED POLY (ETHYLENE TEREPHTHALATE)

J.D. Badia, A. Martinez-Felipe, L. Santonja-Blasco, A. Ribes-Greus*

Instituto Tecnológico de Materiales. Universidad Politécnica de Valencia.

Camino de Vera, s/n, 46022 Valencia (Spain)

*corresponding author: aribes@ter.upv.es

Keywords:

Poly(ethylene terephthalate) (PET); Thermal decomposition; Thermo-oxidative decomposition; Thermogravimetry (TGA); Evolved-Gas Analysis (EGA); 2D-Correlation Infrared Analysis (2D-IR); Kinetic analysis

Abstract:

An exhaustive assessment of the behaviour of virgin and mechanically reprocessed poly (ethylene terephthalate) (PET) facing thermal and thermo-oxidative decomposition processes is presented in this work, as an approach for the energetic valorisation of post-consumer PET goods. Multi-rate linear-non-isothermal thermogravimetric (TGA) experiments under inert (Ar) and reactive (O_2) conditions were performed to virgin PET and its recyclates in order to simulate the thermal behaviour of the materials facing pyrolysis and combustion processes. The release of gases was monitored by Evolved Gas Analysis of the fumes of the TGA experiment, by in-line Fourier-Transform InfraRed (IR) analysis, with the aid of 2D-Correlation IR characterisation. A kinetic analysis methodology, consisting in the combination of six different methods (namely Flynn-Wall-Ozawa, Kissinger-Akahira-Sunose, Vyazovkin, Master-Curves and Perez-Maqueda Criterion along with Coats-Redfern equation) was applied. Its validity for being used for both constant and variable kinetic parameters was discussed. The kinetic model that described both thermal and thermo-oxidative decompositions of PET and its recyclates was of the type A_n: nucleation and growth of gas bubbles in the melt. Novel parameters and functions were proposed to characterize the thermal stability along the reprocessing cycles, as well as the variation of the activation energy and the pre-exponential factor during thermal and thermo-oxidative decompositions. The reliability of a simplified kinetic triplet with constant activation parameters was suitable only under thermal decomposition. The usability of PET after reprocessing showed a threshold in the thermal performance from the second recyclate on. During thermal and thermo-oxidative processes, reprocessed PET behaved similarly to virgin PET, and thus current energetic valorisation technologies could be assimilable for all materials.

1. Introduction

The extended use of poly(ethylene terephthalate) (PET) over the last two decades, mainly in the food packaging sector, is due to its excellent mechanical, chemical, barrier, processing and thermal properties. Consequently, the amount of post-consumed PET present in urban solid waste is high and has to be managed. Among all recovery methods, mechanical recycling represents one of the most successful processes and has received considerable attention due to a number of advantages [1]. The application of protocols [2-7] to simulate the degradation subjected during mechanical recycling has stated that thermo-mechanical degradation induced by means of multiple reprocessing undergoes reactions among end-groups [8] at temperatures above the melting point, which provoke modifications in the oligomeric distribution of PET [6] thus diminishing its performance [9]. Under this perspective, the application of technologies for energetic valorisation such as pyrolysis or controlled combustion can offer an added value to recycled plastics which service lives at good performance parameters have been overcome. With this processes, plastic waste breaks down due to the application of heat to mainly give out highly calorific gaseous products, from which energy can be obtained [1].

Mechanistically, it is widely known that thermal decomposition of PET may occur mainly via (i) intramolecular back-biting, leading to cyclic dimers or trimers, and (ii) via chain scission trough a β-C-H hydrogen transfer reaction, leading to vinyl ester and acid end-groups [10-11]. Other reactions may occur, due to the high reactivity and variety of chemical groups present in PET. It has been reported how this reactions can be enhanced by the presence of aliphatic end-groups in PET oligomeric distribution [12] or by moieties due to deficient drying, even two-folding the hydrolytic reactions at temperatures above the melting [13]. The presence of dyethylene glycol in its formulation may promote thermal decomposition due to enhanced chain flexibility [14]. The complexity of the decomposition mechanisms is patent in the paper reported by Levchik and Weil [10].

The behaviour of polymers submitted to pyrolysis and/or combustion must be kinetically assessed, in order to model the decomposition mechanism, the rate of the reaction and the rest of reaction parameters necessary to predict the product distribution. This knowledge will lead to the selection of the proper reactor, as well as to the optimization of the reactor design and operating conditions. In this sense, Thermogravimetric analysis (TGA) stands out as fast and reliable characterization technique to ascertain a deeper knowledge about the ongoing thermal and thermo-oxidative decomposition of plastics. Furthermore, the study of the evolved gases may complete the picture of the study and predict the major reaction pathways driven during both thermolytic processes. Owing to its cost-effectiveness, reliability to detect main evolved gases, and ease to be incorporated into in-line industrial processes, Fourier Transform Infra-Red (FT-IR) Spectroscopy is an efficient hyphenated technique to monitor the release of gases [15]. As well, the application of 2D-Correlation IR spectroscopy [16-20] can help determine the

sequence of gases released, as well as to distinguish between overlapped bands to identify products evolved due to different reactions.

With regards to experimental procedures, common studies about the thermally-induced decomposition of PET have focused their interest in the characterization of the thermal stability, decomposition mechanisms and the emission of volatile low molecular weight compounds [21], both in inert [22-23] and oxidative [24-25] atmospheres, also considering the influence of additives such as stabilizers or flame-retardants [26]. Concerning theoretical approaches, literature reports indicate that different researchers use different kinetic models and diverse kinetic methodologies to perform their studies and come up to the kinetics of the thermal or thermo-oxidative decompositions, in an attempt to reach the description of pyrolysis and combustion of their polymers, respectively. This fact often provokes debate about which model is more suitable to best represent the system under study [27-28]. With the purpose of overcoming this controversy, a detailed methodology is presented in this work, as well as the suitability of using a simplified kinetic triplet is addressed.

Summing up, the aim of this work was to assess the behaviour of a model polymer (i.e. PET) facing energetic valorisation procedures such as pyrolysis and combustion, in order to develop a methodology transferable to other polymeric materials. Furthermore, the effect of mechanical reprocessing on PET thermal behaviour is addressed as a means to approach the combination of material and energetic valorisations in the treatment of PET wastes. The study was focused in three aspects: (i) the study of the thermal and thermo-oxidative stability; (ii) the control of gases emitted in relationship with the thermolytic mechanisms; and (iii) the kinetic modelling of the energetic valorisation considering both variable and constant activation parameters.

2. Experimental procedures

2.1. Material and mechanical recycling simulation

Poly (ethylene terephthalate) (PET) SEDAPET SP04 was a bottle-grade PET obtained from Catalana de Polimers S.A., Grup LaSeda (Barcelona, Spain) in the form of pellets. Prior to processing, virgin PET (VPET) pellets were dried during 5 h at 160 ºC in a dehumidifier Conair Micro-D FCO 1500/3 (UK), in order to remove as much humidity as possible from the PET flakes. Afterwards, samples were processed by means of injection moulding employing an Arburg 420 C 1000-350 (Germany) injector, single-screw model (diameter Φ=35 mm, length/Φ=23). Successive processing steps were applied under the same conditions. Temperature gradient set from hopper to die was 270, 275, 280, 285 and 280 ºC. Moulds were set at 15 ºC. Cooling time residence was ~ 40 s and total residence time ~ 60 s. Samples were dried before each processing cycle. After injection, a fraction of the samples was kept as test specimen and the rest was ground by means of a cutting mill Retsch SM2000 (UK), which provided pellets of size Φ < 20 mm to be fed back into the recirculation process. Up to five processing cycles were to obtain reprocessed PET (RPET-i, with i cycles: 1-5).

2.2. Simulation of energetic valorisation. Thermogravimetric experiments

Multi-rate linear non-isothermal thermogravimetric (TGA) experiments were carried out by means of a Mettler-Toledo TGA/SDTA 851 (Columbus, OH). Samples weighing ~ 5 mg were heated in an alumina holder with capacity for 70 µL. Experiments were performed from 25 to 900 ºC at different heating rates (β = 2, 5, 7, 10, 12, 15, 17, 20, 25, 30 ºC·min^{-1}), under constant flow of 50 mL·min^{-1} of gas of analysis. An inert Ar atmosphere was used for assessing the thermal decomposition behaviour, whereas an O_2 reactive atmosphere was applied for characterizing the thermo-oxidative decomposition processes of PET and its recyclates. The characterization was performed with the aid of the software STAR^e 9.10 from Mettler-Toledo. Experiments were repeated at least three times, and the averages were considered as representative values.

2.3. Evolved Gas Analysis. Fourier Transform Infrared Analysis hyphenated to Thermogravimetry.

Evolved Gas Analysis (EGA) was applied to fumes released by both thermal and thermo-oxidative processes by means of coupling Fourier-Transform Infrared Analysis (FT-IR) to the TGA. In this case, the TGA analysis was performed by means of a heating rate of 1 ºC·min^{-1}, according to the equipment specifications. Samples weighing ~ 40 mg were heated in an alumina holder with capacity for 900 µL. The flow rate of the carrier gas was set to 25 mL·min^{-1}. The FT-IR gas-phase spectra were collected by a Thermo Nicolet 5700 FT-IR Spectrometer (MA, USA), previously calibrated, from 4000 to 600 cm^{-1} of wavenumber, at a resolution of 4 cm^{-1}. Both transfer line and gas cell were kept at 250 ºC to prevent gas condensation. FT-IR spectra were characterized by OMNIC 7.0 from Thermo Scientific. 16 co-added spectra were recorded every 30 s to assure the accuracy of the temperature scanning.

2.4. Computational assumptions

Kinetic analyses were performed in the conversion degree α range from 0,1 to 0,8 since the main reaction took place in this region. All thermogravimetric data were analyzed using Microsoft® Excel software. Vyazovkin method required the tool Solver® of this mathematical package, by applying Newton method with progressive derivatives, setting an accuracy of 10^{-6} and a tolerance of 10^{-4}. Fitting procedures were performed by means of OriginLab OriginPro 8.0, which uses the Levenberg-Marquardt algorithm [29-30] to adjust the parameter of the fitting values in the iterative procedure. Results are plotted in terms of {average, dev_{max}, dev_{min}}, where dev_{max} = max(data)-average(data), and dev_{min} = average (data)-min(data). Tabulated errors were obtained by dividing the standard deviation by the average of data.

3. Results and discussion

3.1. Studies on the thermal and thermo-oxidative decomposition stability

3.1.1. Decomposition profiles

The thermal performance of virgin and reprocessed PET (VPET, RPET-i, respectively) was initially addressed. The thermogravimetric curves (*TG*) and their first-order derivative curves (*DTG*) were analysed after each reprocessing step at all heating rates β and compared to the *TG* and *DTG* curves of the virgin PET. **Figure 1** shows the influence of the thermal (*TD*) and thermo-oxidative (*TOD*) decomposition processes on the *TG* curve displayed for VPET and RPET-5; the experiments of the other recyclates are omitted for the sake of clarity, but laid between those limiting lines. As usual, higher β lead the thermograms to be shifted to higher temperatures.

Figure 1

The *TD* of PET occurred through a single decay stage, regardless the reprocessing cycle and the β employed for the thermogravimetric analysis. After a long thermostability range (until ~ 380ºC), the material decomposed fast within ~ 380-480ºC, consuming the majority of the mass. Afterwards, the remaining char continuously smoothly decomposed until the end of the experiment, .. The main mass-loss step slightly increased (from 80 to 85%) with each reprocessing step, as shown in **Table 1**, clear effect of a weakened material.

The *TOD* of PET followed a two-step mass-loss process. As expected, the use of an oxidative atmosphere fastened the decomposition of the material until ~ 300ºC, shifting the *TG* curves to lower temperatures in comparison to those obtained using inert atmosphere. Due to thermo-mechanical degradation, the reprocessed material had more potential sites liable to oxidation, as shown in previous studies [6], and therefore in presence of O_2, the difference in thermal stability was larger. In general, the presence of oxygen did not significantly alter the profile of the decomposition, so thus it could be guessed that the chemical reaction that led the main mass-loss was of the same nature under both environments, as also further confirmed by evolved gas analysis. In contrast, the presence of O_2 enhanced the decomposition of the remaining char found in inert conditions, consuming therefore nearly the whole amount of material, since the remaining residue could be considered negligible (~ 0.5%). For further analysis, the two-step thermo-oxidative decomposition was deconvoluted[1] by means of Eq. (1) applied to the *DTG* curve, in order to characterize individually each of the contributions to the overall decomposition:

$$\frac{d\alpha}{dT}(T) = \frac{d\alpha}{dT}\bigg|_{A=0} + \sum_i A_i \cdot \left(1 + e^{-\frac{T-T_i-\frac{W_{1i}}{2}}{W_{2i}}}\right)^{-1} \cdot \left(1 - \left(1 + e^{-\frac{T-T_i-\frac{W_{1i}}{2}}{W_{3i}}}\right)^{-1}\right) \quad (1)$$

---

[1]See example of deconvolution in the supplementary material.

, where α is the conversion degree, A_i and T_i are the amplitude ant peak temperature of each i peak; and w_{1i}, w_{2i}, w_{3i} are dispersion coefficients that adjust the width, asymmetry and skewness of the curves [31]. A posterior integration of the areas under each curve provided the relative importance of each mass-loss step to the overall decomposition. In contrast to studies under inert gas, the thermo-oxidative decomposition took place through a first step that consumed ~77-80 % of mass, followed by a second step with a consumption of the resting ~23-20 %, as showed in **Table 1**.

Table 1

3.1.2. A novel model to functionalise the evolution of the thermal and thermo-oxidative stability at any linear heating rate.

In order to assess the thermal performance under both inert and reactive conditions, the corresponding decomposition onset and endset temperatures (T_{on}, T_{end}) were obtained by a tangential intercept method onto the *TG* curves for the whole process. Likewise, the temperature at the maximum decomposition rate $d\alpha/dT$, i.e. the peak temperature of the *DTG* curve, which is related to the inflection temperature of the *TG* curve (T_P) was also considered for both mass-loss processes. **Figure 2** shows the influence of the heating rate β on the aforementioned temperatures for the case of VPET, tested under Ar (**Fig 2a**) and O_2 (**Fig 2b**). The same trend was shown by all reprocessed PET. Technologist may be interested in finding the relationship between the influence of the heating rate β and the characteristic TGA temperatures to model the thermal behaviour of PET. That would be useful to predict the decomposition temperatures of PET under any β. At fast β, the relationship was almost linear, but it bended when β approached slower values. There are studies [32] that propose linear dependences, but it was higher to nearly 15 ºC·min^{-1} that the tendency got to a linear asymptote. It would be therefore interesting to apply functions to functionalise the thermal decomposition behaviour (*TDB*) of PET under any β. In this sense, Eq. (2), where a, b and k are parameters of the fitting, was applied for virgin and reprocessed PET, at both atmospheres and for the three characteristic temperatures[2].

$$TDB(\beta) = a \cdot \left(1 + b \cdot e^{-k \cdot \beta}\right)^{-1} \qquad (2)$$

With the aim of assessing the influence of thermo-mechanical degradation induced by multiple reprocessing on PET, the use of temperature parameters obtained for a single heating rate are not recommended, since they can be strongly dependent on the experimental settings. In this work, the peak Zero-Decomposition Temperature (ZDT_P), which is the temperature at which *TDB* ($\beta \rightarrow 0$) for the T_P evolution, is proposed, due to its use may attenuate the abovementioned experimental errors. On the other hand, one may be tempted to use the same expression and extrapolate to "infinite" β values, since *TDB* ($\beta \rightarrow \infty$) = a, and then perform *TGA* experiments at high β in order to ease the procedure, but it was observed how a fluctuated. **Fig2c** displays the evolution of ZDT_P along the reprocessing cycles under both thermal *TD* and thermo-oxidative *TOD* decompositions, showing in both cases a decrease due to the weakening of PET backbone due to thermo-mechanical degradation [6]. The change in tendency from

---

[2] See results of fitting in the supplementary material.

VPET→RPET-2 to RPET-3→RPET-5 may indicate the threshold of recycling for the material in terms of thermal performance.

Figure 2

3.2. Evolved Gases Analysis: control of emission.

3.2.1. The use of Fourier-Transform Infrared analysis coupled to Thermogravimetry.

Due to the complexity of the oligomeric distribution of PET [6], different gaseous compounds can be released [14-15, 21]. **Figure 3** shows the *3D/FT-IR* spectra (**Fig 3a-b**) and contour *2D/FT-IR* maps (**Fig 3c-d**) for the thermal decomposition *TD* and thermo-oxidative decomposition *TOD* of virgin PET, along with their *FT-IR* spectra at the maximum decomposition rates (**Fig 3e-f**).The pattern of gases released under inert atmosphere differed from that obtained under oxidative conditions, since PET decomposed in a progressive fashion under Ar, while, under O_2, PET decomposition showed two main releases of gas, according to the two mass-loss stages. A list of the most significant detected gases under both *TD* and *TOD* is given in **Table 2**, with the corresponding vibrational groups and characteristic wavenumbers.

Under inert atmosphere, major observable gases by *FT-IR* were acetaldehyde, carbon monoxide, and carbon dioxide. The presence of peaks in the 1500-1600 cm^{-1} and 800-950 cm^{-1} regions, corresponding to aromatic species could be related to the release of compounds like benzene, benzoic acid or benzaldehyde, among other minor compounds. Due to the small presence of OH groups in the 3400-3800 cm^{-1} region related to acids, which may tend to decarboxylate giving rise to CO_2, and according to the main decomposition mechanisms widely accepted for PET, the release of benzaldehyde was also considered. The aldehydic peaks corresponding to acetaldehyde and benzaldehyde appeared overlapped, and therefore a deconvolution procedure (see detail in **Fig 3c-Ar**) by means of Lorentzian curves was applied in different characteristic stretching vibration regions (H-C=O; C=O and C-O). From each set of curves, benzaldehyde bands were those shifted to lower wavenumbers in comparison to those of acetaldehyde, due to the interaction with the aromatic group. As well, small traces of water and methane could be taken into account.

Under oxidative conditions, the first decomposition stage produced similar compounds to those obtained in inert conditions, and it could therefore be assigned to the pyrolytic decomposition of PET, severely due to thermal conditions. As main differences attributable to the action of O_2, a major predominance of acetaldehyde to a detriment of benzaldehyde was observed, as well as a minor production of CO, being the release of CO_2 remarkably prevalent. In contrast to what happened under inert conditions, at higher temperatures, the thermo-oxidative decomposition of PET released CO_2, due to the combustion of the remaining char.

Figure 3 – Table 2

3.2.2. 2D-Correlation Infra-Red Spectroscopy (2D-IR) studies

9

2D-Correlation Infra-Red Spectroscopy (*2D-IR*) was applied to the first stages of both thermal (*TD*) and thermo-oxidative (*TOD*) decompositions, which gave the same profile of results (**Figure 4**), thus confirming that the same mechanisms took place.

The synchronous spectrum in the 4000-600 cm^{-1} region (**Fig 4a**) showed the predominant auto-peaks of the main groups [υ(C=O), υ(CHO), υ(C-O), δ(CH$_3$), υ(C$\equiv$O) and υ_{as}(O=C=O)], with their corresponding positive cross-peaks which indicated the same behaviour of appearance for all bands. The asynchronous spectrum in the 2900-1600 cm^{-1} region (**Fig 4b**) showed four major negative cross peaks at (2356, 1760), (2356, 1724), (2106, 1760) and (2106, 1724), which indicated that both acetaldehyde and benzaldehyde were released before CO and CO$_2$. These results are in agreement with the general mechanism of thermal decomposition in which a first release of an aldehydic compound due to back-biting intramolecular esterification leaves an acid-terminated chain which may continue back-biting or decarboxylating to give out carbon oxides. Between these carbon oxides, the release of CO started before the appearance of CO$_2$, as shown by the asynchronous spectrum in the 2400-2000 cm^{-1} region (**Fig 6c**). On the other hand, the positive cross-peaks at (1760, 1724), (2740, 2690) and (1127, 1081) in the asynchronous spectrum in the wavenumber regions 1900-1700 cm^{-1}(υ(C=O)), 2900-2400 cm^{-1}(υ(CHO)) and 1600-800 cm^{-1}(υ(C-O)), shown at **Fig 4d-e-f**, clearly stated that acetaldehyde was evolved before benzaldehyde. As can be seen at the contour *2D/FT-IR* map of thermal decomposition (**Figure 3**),when aldehydic compounds disappeared, CO and CO$_2$ still evolved at higher temperatures, being CO$_2$ the last released compound. Summing up, in comparison with the general thermolytic mechanisms of PET, one can figure out that both *TD* and *TOD* were initiated by transesterification reactions, giving preference to the formation of acetaldehyde.

Homolytic scissions took place simultaneously during *TD* and continued at high temperatures. During *TOD*, homolysis disabled transesterification reactions at high temperatures, giving rise to the combustion of the material to mainly give CO$_2$. Thus, the establishment of proper operation temperatures might control the nature of the gases released.

It was remarkable that the behaviour described was valid not only for virgin PET but also for the rest of reprocessed materials. Despite the material suffers chemical modifications in its structure and morphology due to thermo-mechanical degradation induced by mechanical recycling [6], at temperatures above the melting, the polymer decomposed in a similar fashion. Gram-Schmidt plots of evolved gases ,not shown for conciseness, gave alike spectra under each atmosphere. This fact is very important, since it means that the same facilities used to control the emission of gases for virgin PET could be adapted to its recyclates with no extra cost.

Figure 4

3.3. Thermal and thermo-oxidative decomposition kinetics

10

In the attempt to develop a model for plastic thermal and thermo-oxidative decompositions in full-scale systems, the main purpose is to describe the behaviour of polymers in terms of an intrinsic kinetics, in which heat and mass transfer limitations are not included. General kinetic models are proposed in literature for plastics and biomasses. These models do not take into account the rigorous and exhaustive description of the chemistry of thermal decomposition of polymers and describe the process by means of a simplified reaction pathway. It is widely known that each single reaction step considered is representative of a complex network of reactions [33].

Khawan and Flanagan [34] reviewed the relationship between the theoretical decomposition mechanisms and their mathematical models, the so-called kinetic functions *f(α)*.Regardless the competitive chemical mechanisms involved in the thermal and thermo-oxidative decomposition of PET, the possibility of modelling its thermal performance in terms of an intrinsic kinetics will help technologist to approach the experimental settings of energetic valorisation processes such as pyrolysis or combustion. For this purpose, a methodology[3] that combined (i) isoconversional methods [35-39], (ii) use of Master-Plots [40], and (iii) *Perez-Maqueda et al*. criterion [41] was carried out. It is common to establish a set of activation energy (*Ea*), pre-exponential factor (*A*) and kinetic model (*f(α)*) to compose the so-called kinetic triplet, being both *Ea* and *A* considered constant for easier calculations. In contrast, the variation of the kinetic parameters with the conversion degree *α* was considered in this paper, with the aim of modelling the *TD* and *TOD* processes with more accurate precision.

3.3.1. Studies on the apparent activation energy

The *Flynn-Wall-Ozawa* (*FWO*) [35-36], *Kissinger-Akahira-Sunose* (*KAS*) [37-38] and *Vyazovkin* (*VYZ*) [39] methods were firstly applied to evaluate the dependence of the apparent activation energy (*Ea*) with the conversion degree *α*, avoiding the interference of an initial assumption of a specific kinetic model. **Figure 5** shows the results of the application of the isoconversional methods on the thermogravimetric data for virgin and reprocessed PET. **Fig. 5a** shows an example for the goodness of *FWO* method, since well-defined straight lines were obtained, from which slope the apparent activation energy was found for each conversion degree (Ea_{α_FWO}). The evolution of Ea_{α_FWO} with *α* is shown in **Fig. 5b**, along with the evolution of the apparent activation energies obtained by *KAS* (Ea_{α_KAS}) and *VYZ* (Ea_{α_VYZ}) methods. The regression coefficient of the linear *FWO* and *KAS* methods was far above the 95 % of confidence for experiments under Ar, as shown in the inset of **Fig. 5b**, whereas this coefficient dropped between an acceptable 92-96% range for experiments performed under O_2. *VYZ* results accomplished the minimum tolerance set at 5%, as pointed out in the experimental section. It has to be stressed that for all materials at both tested environments, the results obtained by the three methods were pretty similar, but they are not shown for the sake of conciseness. The variation of the average apparent activation energy obtained by the isoconversional methods (Ea_{iso_α}) is shown for virgin PET and its five successive recyclates thermally decomposed under inert and oxidative atmospheres in **Figs. 5c** and **5d**, respectively. Two different behaviours could be distinguished for the thermal decomposition (*TD*), where VPET and RPET-1,2

---

[3] Mathematical description ok kinetic models given in the supplementary material.

showed an initial decrease approaching a constant value at α > 0.3, whereas RPET-3,4-5 described an increasing slope from the beginning of the decomposition. On the other hand, during the thermo-oxidative decomposition (*TOD*), all materials showed the same increasing trend for Ea_{iso_a}. According to the shape of the curves [42], the *TD* of VPET, RPET-1,2 had reversible stages, probably due to instantaneous reactions between short-chain acidic and alcoholic compounds to form esteric structures which immediately decomposed. Due to further thermo-mechanical degrading action, these reactions might had been disabled for RPET-3, 4, 5, where the parallel formation of aldehydic compounds and carbon oxides might provoke the continuous increase of Ea_{α}. The presence of O_2 would also act promoting the volatilization reactions, without allowing recombination.

It was found that Eq. (3) fitted the experimental data for all materials at both atmospheric conditions:

$$Ea(\alpha) = Ea^I + (Ea^{II} - Ea^I) \cdot e^{-\left(\frac{\alpha}{p}\right)} \qquad (3)$$

, where Ea^I and Ea^{II} are parameters that can be obtained from the intercept at α = 0 and in the asymptote, giving an idea of the amplitude of decomposition, and *p* is a power to correct the curvature of the function. This equation allows modelling both increasing and decreasing tendencies, also adapting to acceleration and deceleration phenomena[4]. These parameters were useful for the characterization of the thermal behaviour of PET and its recyclates, where *p* values close to 0 indicated an *Ea* becoming almost constant, while higher *p* (close to 1) approached linear tendencies. Taking into account the whole α range, under inert conditions, an *Ea* increase was observed from VPET to RPET-1,2, therefore indicating higher energy to trigger the decomposition of the materials, probably due to the recombination of the chains scissored during reprocessing, as suggested in a previous study [6], where the formation of cyclic PET oligomers from the loss of an extra glycol unit in cyclic oligomers was shown. Afterwards, a general decrease down to orders lower than those shown by VPET was obtained, as a weakening effect of the thermo-mechanical degradation induced to PET recyclates. The presence of more linear hydroxyl- and carboxyl- terminated linear species [6], more liable to temperature, could trigger and propagate the thermal decomposition (*TD*) reactions in a faster fashion and therefore less energy would be needed. With regards to the behaviour of PET facing thermo-oxidative decomposition (*TOD*), all recyclates showed a general decrease in their *Ea*, in two steps: from VPET to RPET-1,2; and then to RPET-3,4,5. As expected, the *TOD* of all materials would be initially achieved with less energy than the *TD*, due to the added influence of the oxidative ambient, as can be checked at **Figure 5**. The presence of O_2 attacked the structure of PET disabling the thermal stability mechanisms of its recyclates therefore showing a progressive degradation throughout the reprocessing cycles. From a cost-effective point of view, taking into account the energetic demand of each process, the combustion of reprocessed PET might result more interesting than its pyrolysis, specially bearing in mind that the thermal performance of PET is lost after the second recyclate.

Figure 5

---

[4] See results of fitting in the supplementary material.

3.3.2. Evaluation of the kinetic model

In order to continue with the kinetic methodology, the next step was the assessment of the kinetic model. The Master Plots based on the differential form of the generalized kinetic equation were used for the common theoretical functions[5] for nucleation, reaction and diffusion [34]. Eq. (4) was used to select the kinetic model that better fitted the experimental data, taking into account the experiments at all heating rates β, where MP_t and MP_e were the theoretical and experimental master plots of the kinetic functions in their differential form. The model that provided a minimum value of Φ was of the type A_n, that is, growth of previously formed nuclei, for virgin PET and all its recyclates under both environments. **Figure 6** shows the comparison of Master-Plots as an example of the suitability of the model A_n to describe the behaviour of both thermal and thermo-oxidative decompositions of VPET and RPET-1 along the studied α range for the experiment at 5 ºC·min^{-1}.

$$\Phi(f_t, \alpha) = \sum_\beta \left| \quad \Phi(f_t, \alpha) = \sum_\beta \left(\sum_\alpha [MP_t(\alpha) - MP_e(\alpha)]^2 \right), \Delta\alpha = 0.025 \right. \tag{4}$$

Figure 6

3.3.3. Closing the kinetic triplet. Determination of the pre-exponential factor

Taking into account that a suitable kinetic triplet should fulfil the *Perez-Maqueda et al* criterion (*P-Mc*); that is, the independence of the activation parameters Ea, A on the heating rate β, the minimization of ξ in Eq. (5) would provide the best n for the modelization, and thereafter provide the most accurate A, by averaging the A_β obtained from the intercept at y=0 of *Coats-Redfern* [43] expression (Eq. 6), since among the different methods that calculate the Ea from a given $f(\alpha)$, this one was demonstrated to offer precise results [44]. The calculations were performed taking into account all h experiments with different β, and the integral form of the model A_n.

$$\xi(n, \alpha) = \sum_i^h \left| \quad \xi(n, \alpha) = \sum_i^h \left| (-R) \cdot \frac{d}{dT} \left(\frac{ln\left(\beta_i \cdot T^{-2}(-\ln(1-\alpha))^{\frac{1}{n}}\right)}{T^{-1}} \right) - Ea_\alpha \right| \right. \tag{5}$$

$$\left[ln \frac{\beta \cdot (-\ln(1-\alpha))^{\frac{1}{n}}}{T^2} \right]_y = ln \frac{A_\beta \cdot R}{Ea_\beta} + \frac{Ea_\beta}{R} \cdot \left[\frac{1}{T} \right]_x \tag{6}$$

---

[5] See common kinetic functions used in solid-state decomposition kinetics.

Table 3 reports the *n* values in which the experimental data laid, which range was approached by the application of the differential Master-Plots (*MP$_f$*), in comparison with the averaged *n* value analytically obtained by the application of *Perez-Maqueda et al.* criterion (*P-M$_C$*), which offered nearly constant *n* values with a fairly small deviation for the thermal decomposition and acceptable values with error margins < 5.5 % for the thermo-oxidative decomposition. The consistency of the results given by both methods is remarkable. Subsequently, the pre-exponential factor was calculated. **Figure 7** shows the evolution of *lnA$_\alpha$* for virgin PET and its recyclates under inert and reactive atmospheres. Deviation among experiments performed at different heating rates was negligible therefore confirming the goodness of *A$_n$* as kinetic model. Finally, in order to mathematically describe the variation of the pre-exponential factor with α, the evolution of *lnA$_\alpha$* was also fitted to Eq. (3), by changing *Ea* into *lnA*, strengthening the suitability of Eq. (3) as modelling function for the pre-exponential factor [6], as can be also checked at **Figure 7**.

Figure 7 – Table 3

3.3.4. Effects of reprocessing on the thermal and thermo-oxidative decomposition kinetics of PET

The kinetic methodology proposed in this paper permitted to accurately describe the kinetic model for explaining the thermal and thermo-oxidative decomposition behaviours of virgin PET and successive recyclates, being the variation of the kinetic parameters specifically determined along the decomposition process. According to the results, the kinetic model that better explained both processes was a nucleation and growth model (*A$_n$*). Despite this kind of model is quite common in crystallization processes, for thermal and thermo-oxidative decompositions, it is scarcely reported [45-49]. However, in these studies, the controversy of the relationship between the mathematical models and the physical mechanisms was remarkable, as well as different assumptions such as constant *Ea* were taken. Even more, according to Mamleev et al. [50], the initial stage of polymer decomposition is often accompanied by the melting, where the control of the process is mainly run by the formation of gas phase inside the molten polymer, and thus by nucleation and nuclei growth in an heterogeneous medium. Due to the low heating rate *β* used in the case of non-isothermal decompositions, low *Ea$_\alpha$* values controlled the formation of nuclei, while a rapid increase in *Ea$_\alpha$* controlled the nuclei growth [51]. This fact also pointed out the weakening of the material due to thermo-mechanical degradation induced by multiple processing, remarkably up to the second recyclate, where the differences in behaviour among recycled materials were less noticeable. Therefore, under inert conditions, the formation of nuclei was important at the initial steps of decomposition for VPET, RPET-1,2, while the release of growing gas bubbles in the melt ruled the decomposition from the beginning for the rest of recyclates. Under an oxidative atmosphere, the decomposition of all materials was ridden by an increasing *Ea$_\alpha$* throughout the process, since the liability of PET to react with O_2 induced potential sites where the reactions of gas formation could take place. The fact that the kinetic component inherent to the material, i.e. the kinetic model, did not change is very interesting, which indicate that technologists may transfer the procedures used for the pyrolysis and

---

[6] See results of fitting in the supplementary material.

combustion of virgin PET to its recyclates, by only taking into account the kinetic components related to the temperature in relation with the variation in apparent activation energy throughout the decomposition processes.

3.3.5. Validity of a simplified kinetic triplet (SKT)

Most of the studies found in the literature report the parameters of the kinetic triplet (Ea, A) as constant values along the whole decomposition process. The possibility of approaching the behaviour of the thermal and thermo-oxidative decomposition processes by a simplified kinetic triplet (*SKT*) would fasten the calculations, and therefore ease the decision of the operational parameters for pyrolysis and combustion. In this section, the validity of using the *SKT* was assessed for the case of PET and its successive recyclates. **Table 4** shows the average apparent activation energies obtained by the aforementioned isoconversional methods (Ea_{FWO}, Ea_{KAS} and Ea_{VYZ}), as well as the average activation energy (Ea_{iso}) susceptible for being used in further calculations. The Ea_{α} used along the previous sections may be therefore now assumed constant along the α range of thermal decomposition (*TD*), since deviations were within a 5 %, whereas for thermo-oxidative decomposition(*TOD*), the average values, though pretty similar among isoconversional methods, offered a big dispersion along the conversion α range (17-29%). Care must be taken when interpreting Ea average data, since one could think that the same amount of energy would trigger the decomposition in both inert and reactive atmospheres, when actually, in the case of virgin PET, ca. 200 kJ·mol^{-1} were needed under Ar, in contrast to ca. 140 kJ·mol^{-1} under O_2 at lower α, as shown in **Fig. 5c** and **5d**.

Eq. (4) was applied to test the accuracy of the theoretical kinetic functions to fit the experimental data, where now Ea_{α} was taken as constant parameter Ea_{iso}. The model that better fitted both *TD* and *TOD* was of the type A_n, in agreement with the previously obtained results with variable Ea. In order to complete the simplified kinetic triplet (*SKT*), the *Pérez-Maqueda et al.* criterion (*P-M$_C$*) was considered in combination with *Coats-Redfern* expression (*C-R*). After the computation of the n, the calculation of lnA was straightforward from the intercept at the origin of Eq. (6) for each β. The results of this procedure are reported at **Table 5** for virgin PET and its recyclates, at both tested atmospheres. While for the *TD*, all obtained values lay within a narrow experimental error and provide similar n to those obtained in the previous section, in the case of *TOD*, the deviation margins were wider and the n values quite different. This was due to the experimental error of assuming the Ea constant, which was transmitted along the rest of the calculations. **Figure 7** represents the application of the *P-M$_C$* with *C-R* method for RPET-2 as an example of the assessment of the suitability of the different *SKT* to be used in further analyses. It can be seen how for *TD* studies, all points lay on the same line, fact that occurred for the rest of materials, regardless the β employed. Contrarily, the points obtained for the *TOD* did not lie on the same line, thus confirming that the *SKT* shown was merely artifactual and therefore its use should be avoided. In this case, only the calculations shown in the previous section considering variation of kinetic parameters shall be operative.

Figure 7-Tables 4-5

4. Conclusions

The thermal behaviour of virgin (VPET) and multiple-reprocessed (RPET-i) poly (ethylene terephthalate) under pyrolysis and combustion was systematically simulated by Thermogravimetric analysis coupled to Fourier-Transform Infrared Analysis, and with the aid of 2D-Correlation Infrared Spectroscopy. The proposed methodology comprised the assessment of the thermal and thermo-oxidative stability, the control of volatiles and the kinetics of decomposition.

Concerning the thermal and thermo-oxidative stability, a novel model, called Thermal Decomposition Behaviour, i.e. TDB (β), was applied to stress the use of the theoretical peak Zero-Decomposition Temperature as a reliable indicator for assessing the weakening of PET due to mechanical reprocessing.

The thermal decompositions of VPET and RPET-i mass-losses were driven by one stage of decomposition that mainly released acetaldehyde and, with less presence benzaldehyde, followed by a release of CO and CO_2, being the emission of the latter followed at higher temperatures. On the other hand, the thermo-oxidative decomposition occurred through a double mass-loss profile. During the first stage, assignable to the bulk pyrolysis, mainly acetaldehyde was released, while throughout the second one, a noticeable production of CO_2 was assessed. The same gas emission profile than that given by VPET was encountered for all recyclates, thus current gas control facilities used for VPET could be assimilated for all RPET-i.

A kinetic analysis methodology consisting in the combination of six different methods (namely Flynn-Wall-Ozawa, Kissinger-Akahira-Sunose, Vyazovkin, Master-Curves and Perez-Maqueda Criterion along with Coats-Redfern equation) was comprehensively developed for the mathematical description of the thermal and thermo-oxidative decomposition of virgin PET and its successive recyclates throughout the whole conversion (α) range. The variation of Ea and A was taken into account and a function was proposed to model their variation along α. The kinetic model was of the type A_n: nucleation and growth, which gave importance to the formation of gas bubbles in the melt. The validity of a simplified kinetic triplet was also assessed, being its use advisable when the activation energy could be considered constant within a narrow confidence interval, as in the case of pyrolysis, but not for the case of combustion.

Regarding the usability of PET recyclates after reprocessing, a change in tendency shown by thermal stability and thermal activation parameters from the second to the third recyclate may indicate the threshold of reprocessing cycles achievable by PET within a certain thermal performance. In general, lower temperatures and energies were necessary to run thermo-oxidative decomposition of PET. Focusing on each process, under Ar, RPET-1 andRPET-2 needed more energy to decompose than VPET, being then reduced for the rest of recyclates; whereas under O_2, the decomposition of all recyclates was overcome at lower Ea than that of VPET. All the considerations shown in the work may provide technologist with plausible indicators for the selection of the adequate recovery option of poly (ethylene

terephthalate). The applicability of the presented methodology may be transferred to the plastic waste management of other polymeric materials.

17

References

1. S.M. Al-Salem, P. Lettieri, J. Baeyens, Recycling and recovery routes of plastic solid waste (PSW): A review, Waste management, 29 (2009) 2625-2643.

2. E. Strömberg, S. Karlsson, The design of a test protocol to model the degradation of polyolefins during recycling and service life, Journal of Applied Polymer Science, 112 (2009) 1835-1844.

3. F. Vilaplana, A. Ribes-Greus, S. Karlsson, Degradation of recycled high-impact polystyrene .Simulation by reprocessing and thermo-oxidation. Polymer Degradation and Stability, 91 (2006) 2163-2170.

4. F. Vilaplana, A. Ribes-Greus, S. Karlsson, Changes in the micro-structure and morphology of high-impact polystyrene subjected to multiple processing and thermo-oxidative degradation. European Polymer Journal, 43 (2007) 4371-4381.

5. J.D. Badia, F. Vilaplana, S. Karlsson, A. Ribes-Greus, Thermal analysis as a quality tool for assessing the influence of thermo-mechanical degradation on recycled poly(ethylene terephthalate), Polymer Testing, 28 (2009) 169-175.

6. J.D. Badia, E. Strömberg, A. Ribes-Greus, S. Karlsson, A statistical design of experiments for optimizing the MALDI-TOF-MS sample preparation of polymers. An application in the assessment of the thermo-mechanical degradation mechanisms of poly (ethylene terephthalate). Analytica Chimica Acta 692 (2011) 85-95

7. J.D. Badia, E. Strömberg, A. Ribes-Greus, S. Karlsson, Assessing the MALDI-TOF MS sample preparation procedure to analyze the influence of thermo-oxidative ageing and thermo-mechanical degradation on poly (lactide). European Polymer Journal, 47 (2011) 1416-1428

8. F. Samperi , C. Puglisi, R. Alicata , G. Montaudo, Thermal degradation of poly(ethylene terephthalate) at the processing temperature. Polymer Degradation and Stability, 83 (2004) 3-10.

9. F. Awaja, D. Pavel, Recycling of PET. European Polymer Journal, 41 (2005) 1453-1477.

10. S. V. Levchick, E. D. Weil, A review on thermal decomposition and combustion of thermoplastic polyesters. Polymers for Advanced Technologies, 15 (2004) 691-700.

11. G. Montaudo, C. Puglisi, F. Samperi, Primary thermal degradation mechanisms of PET and PBT. Polymer Degradation and Stability, 42 (1993) 13-28.

12. F. Villain, J. Coudane, M. Vert, Thermal degradation of poly(ethylene terephthalate) and the estimation of volatile degradation products, Polymer Degradation and Stability,43 (1994) 431-440.

13. K. S. Seo, J.D. Cloyd, Kinetics of hydrolysis and thermal degradation of polyester melts, Journal of Applied Polymer Science, 42 (1991) 845-850.

18

14. B.J. Holland, J.N. Hay, The thermal degradation of PET and analogous polyesters measured by thermal analysis–Fourier transform infrared spectroscopy. Polymer, 43 (2002) 1835-1847.

15. R. Kinoshita, Y. Teramoto, T. Nakano, H. Yoshida, Thermal degradation of polyesters by simultaneous TGA-DTA/FT-IR analysis. Journal of Thermal Analysis, 38 (1992) 1891-1900.

16. I. Noda, Two-Dimensional Infrared (2D IR) Spectroscopy: Theory and Applications, Applied Spectroscopy, 44 (1990) 550-561

17. I. Noda, Recent advancement in the field of two-dimensional correlation spectroscopy. Journal of Molecular Structure, 883-884 (2008) 2-26.

18. I. Noda, Generalized Two-Dimensional Correlation Method applicable to Infrared, Raman, and other types of Spectroscopy. Applied Spectroscopy, 47 (1993) 1329-1336.

19. I. Noda, Recent developments in two-dimensional infrared (2D IR) correlation spectroscopy. Applied Spectroscopy, 47 (1993) 1317-1323.

20. X. Dou, B. Yuan, H. Zhao, G. Yin, Generalized two-dimensional correlation spectroscopy - Theory and applications in analytical field. Science in China Serie B: Chemistry, 47 (2004) 257-266.

21. M. Dzieciol, J. Trzeszczynski, Studies of temperature influence on volatile thermal degradation products of poly(ethylene terephthalate), Journal of Applied Polymer Science, 69 (1998) 2377-2381.

22. B. Saha, A.K. Groshal, Thermal degradation kinetics of poly(ethylene terephthalate) from waste soft drink bottles. Chemical Engineering Journal, 111 (2005) 39-43.

23. B. Saha, A. K. Maiti, A. K. Ghoshal, Model-free method for isothermal and non-isothermal decomposition kinetics analysis of PET sample, Thermochimica Acta, 444 (2006) 46-52.

24. I. Martín-Gullón, M. Esperanza, R. Font, Kinetic model for the pyrolysis and combustion of poly-(ethylene terephthalate) (PET). Journal of Analytical and Applied Pyrolysis, 58-59 (2001) 635-650.

25. J. Moltó, R. Font, J.A. Conesa, Kinetic model of the decomposition of a PET fibre cloth in an inert and air environment, Journal of Analytical and Applied Pyrolysis, 79 (2007) 289-296.

26. S. V. Levchik, E.D. Weil, Flame retardancy of thermoplastic polyesters—a review of the recent literature, Polymer International, 54 (2004) 11-35.

27. A.K. Galwey, What can we learn about the mechanisms of thermal decompositions of solids from kinetic measurements? Journal of Thermal Analysis and Calorimetry, 92 (2008) 967-983.

28. A. K. Galwey, M. E. Brown, Solid-state decompositions - stagnation or progress? Journal of Thermal Analysis and Calorimetry, 60 (2000) 863-877.

29. K. Levenberg, A method for solution of certain non-linear problems in least squares, Quaterly of Applied Mathematics, 2 (1944) 164-168.

30. D. W. Marquardt, An algorithm for the least-squares estimation of non-linear parameters. SIAM Journal of Applied Mathematics, 11 (1963) 431-441.

31. L. Santonja-Blasco, R. Moriana, J.D. Badía, A. Ribes-Greus, Thermal analysis applied to the characterization of degradation in soil of polylactide: I. Calorimetric and viscoelastic analyses. Polymer Degradation and Stability, 95 (2010) 2185-2191.

32. B. Liu, X. Zhao, X. Wang, F. Wang, Thermal degradation kinetics of poly(propylene carbonate) obtained from the copolymerization of carbon dioxide and propylene oxide. Journal of Applied Polymer Science, 90 (2003) 947-953.

33. B. Wunderlich, Thermal analysis of polymeric materials. Springer, Berlin, 2005.

34. A. Khawan, D. R. Flanagan, Solid-State Kinetic Models: Basics and Mathematical Fundamentals. Journal of Physical Chemistry B, 110 (2006) 17315-17328.

35. J. H. Flynn, L. A.Wall, A quick, direct method for the determination of activation energy from thermogravimetric data. Journal of Polymer Science, 4 (1966) 323-342.

36. T. Ozawa, Kinetic analysis of derivative curves in thermal analysis. Journal of Thermal Analysis, 2 (1970) 301.

37. C. D. Doyle, Series approximations to the equation of thermogravimetric data., Nature, 207 (1965) 209.

33. H. E. Kissinger, Reaction kinetics in differential thermal analysis. Analytical Chemistry, 29 (1957) 1702-1706.

38. T. Akahira, T. Sunose, Trans. Joint Convention of Four Electrical Institutes, Paper No. 246 Research Report/ Chiba Institute of Technology, Scientific Technology, 16 (1971) 22-31.

39. S. Vyazovkin, D. Dollimore, Linear and non-linear procedures in isoconversional computations of the activation energy of non-isothermal reactions in solids. Journal of Chemical Information and Modelling, 36 (1996) 42-45.

40. F.J. Gotor, J.M. Criado, J. Málek, N. Koga, Kinetic Analysis of Solid-State Reactions: The universality of Master Plots for Analyzing Isothermal and Non-Isothermal Experiments., Journal of Physical Chemistry A, 104 (2000) 10777-10782.

41. L. A. Pérez-Maqueda, J. M. Criado, F. J. Gotor, J. Málek Advantages of combined kinetic analysis of experimental data obtained under any heating profile. Journal of Physical Chemistry A, 106 (2002) 2862-2868.

20

42. S. Vyazovkin, A. Lesnikovich, An approach to the solution of the inverse kinetic problem in the case of complex processes: Part 1. Methods employing a series of thermoanalytical curves, ThermochimicaActa, 165 (1990) 239-280.

43. A. W. Coats, J. P. Redfern, Kinetic analysis from thermogravimetric data. Nature, 68 (1964) 4914.

44. L. A. Pérez-Maqueda, P. E. Sánchez-Jiménez, J.M. Criado, Kinetic analysis of solid-state reactions: precision of the activation of the activation energy calculated by integral methods. International Journal of Chemical Kinetics, 37 (2005) 658-666.

45. S. T. Stoeva, K. Gjurova, M. Zagorcheva, Thermal analysis study on the degradation of the solid state chlorinated poly(ethylene). Polymer Degradation and Stability, 67 (2010) 117-128.

46. L. Li, C. Guan, A. Zhang, D. Chen, Z. Qing, Thermal stabilities and the thermal degradation kinetics of polyimides. Polymer Degradation and Stability, 84 (2004) 369-373.

47. J.T. Sun, Y.D. Huang, G.F. Gong, H.L. Cao, Thermal degradation kinetics of poly(methylphenylsiloxane) obtaining methacryloyl groups., Polymer Degradation and Stability, 91 (2005) 339-346.

48. G.Grausea, J. Ishibashia, T. Kamedaa, T.Bhaskarb ,T. Yoshioka, Kinetic studies of the decomposition of flame retardants containing high-impact polystyrene. Polymer Degradation and Stability, 95 (2010) 1129-1137.

49. J.D. Badía, L. Santonja-Blasco, R. Moriana, A. Ribes-Greus, Thermal analysis applied to the characterization of degradation in soil of polylactide: II. On the thermal stability and thermal decomposition kinetics. Polymer Degradation and Stability,95 (2010) 2192-2199.

50. V. Mamleev, S. Bourbigot, M. L. Bras, S. Duquesne, J. Sesták, Modelling of nonisothermal kinetics in thermogravimetry. Physical Chemistry Chemical Physics, 2 (2000) 4708-4716.

51. S. Vyazovkin, C. A. Wight, Kinetics of Thermal Decomposition of Cubic Ammonium Perchlorate. Chemistry of Materials, 11 (1999) 3386.

THERMAL AND THERMO-OXIDATIVE STABILITY OF REPROCESSED POLY (ETHYLENE TEREPHTHALATE)

CAPTIONS TO FIGURES

Figure 1. Thermogravimetric curves of virgin PET and its fifth recyclates under thermal and thermo-oxidative decompositions. Upper: full scale; middle: details of onset of decompositions; lower: detail of endset of decompositions

Figure 2. Thermal stability assessment: Fitting of TDB for the evolution of the characteristic thermogravimetric temperatures at inert (a) and reactive (b) conditions; (c) Evolution of the peak Zero-Decomposition temperature along the reprocessing cycles.

Figure 3. Results from TGA/FT-IR analysis: 3D/FT-IR (a, b) , contour 2D/FT-IR (c,d) and FT-IR spectra at the maximum of decomposition (e,f) plots for the thermal (a,c,e) and thermo-oxidative (b,d,f) decompositions of virgin PET.

Figure 4. 2D-IR correlation spectra of the thermal decomposition of virgin PET at selected wavenumber regions (see text for details).

Figure 5.Application of isoconversional methods for virgin PET. (a) An example of FWO method for experiments under Ar; (b) Ea evolution with the conversion degree evaluated by FWO, KAS and VYZ methods (inset: regression coefficients of fittings); (c) Effect of recycling on the Ea evolution of PET under Ar atmosphere; (d) Idem to (c) but under O_2 atmosphere. Note: In (c) and (d) the solid lines represent the fitting of the proposed equation to the experimental *Ea* variation.

Figure 6.Master-Plots in the differential form for virgin (hollow) and first PET recyclate (full) at 5 ºC•min-1 for both environments. Kinetic models: A_n (nucleation and growth, solid black lines), F_n (n-order reactions, solid grey lines), R_n (reaction-controlled, pointed lines), D_n (diffusion-controlled, dashed lines)

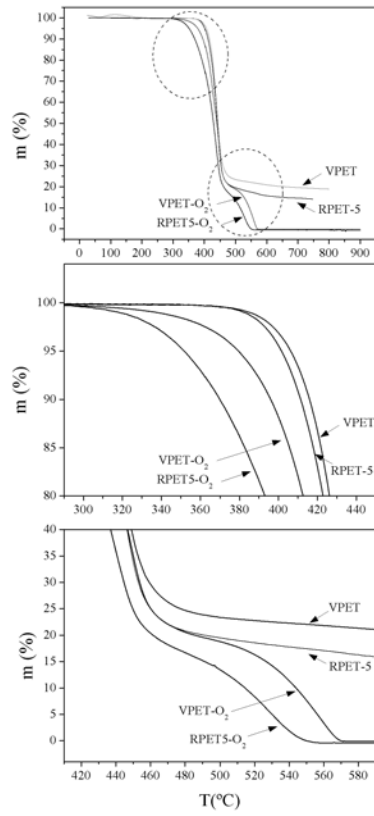Figure 7. Application of Pérez-Maqueda et al criterion for the simplified kinetic triplets.
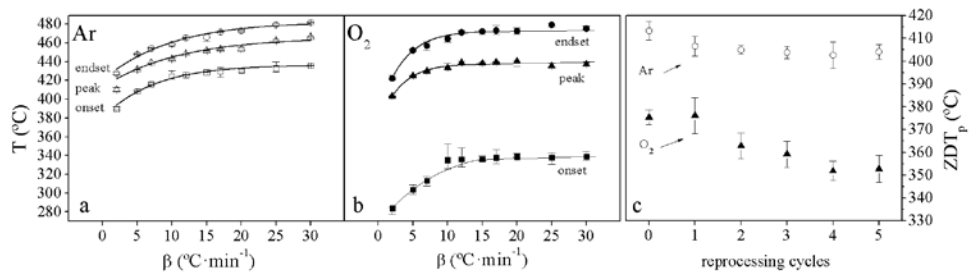
FIGURE 1

FIGURE 2

FIGURE 3

25
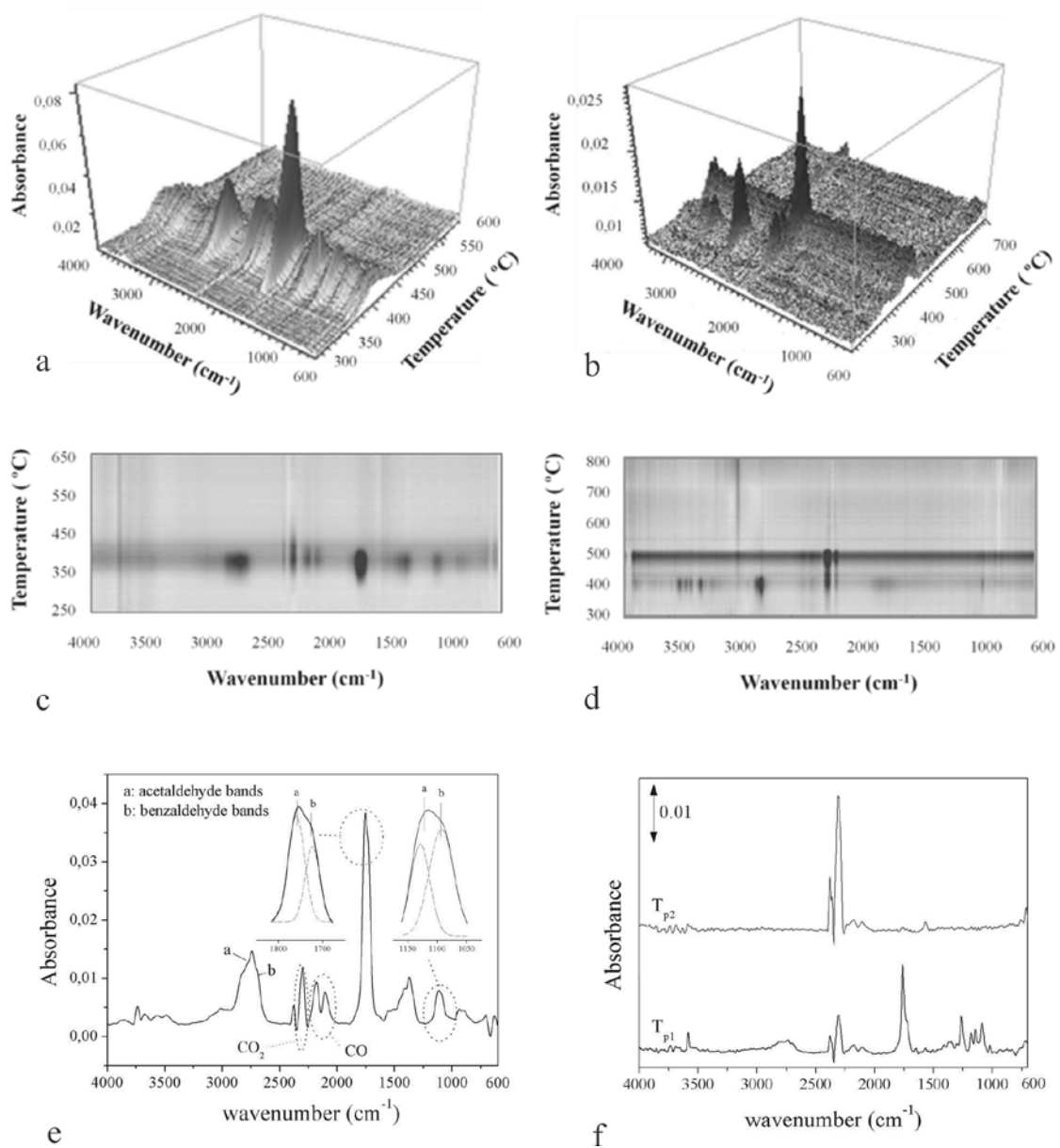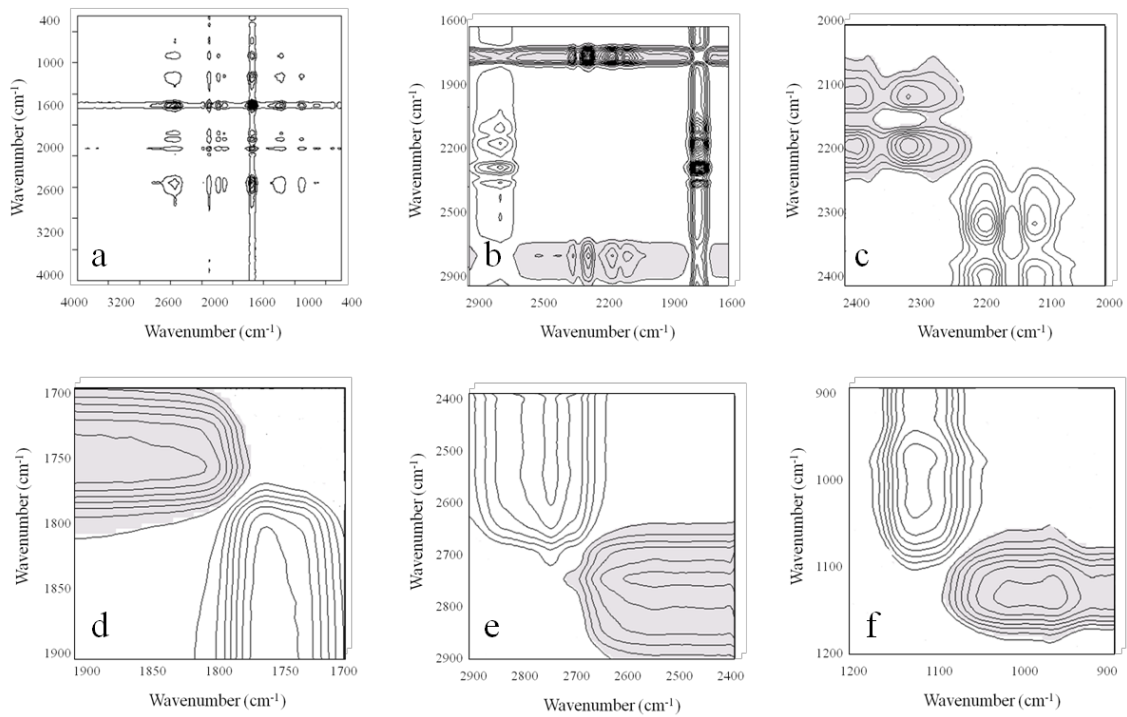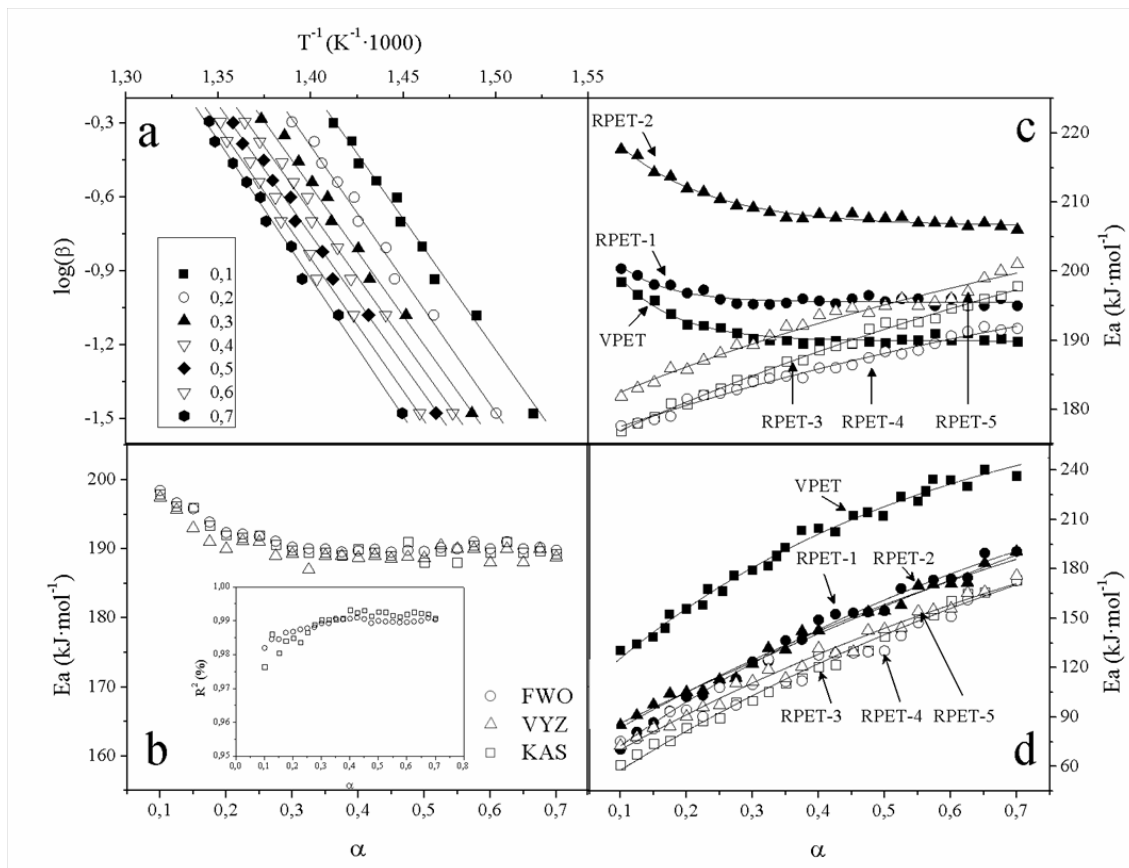
FIGURE 4

FIGURE 5

FIGURE 6
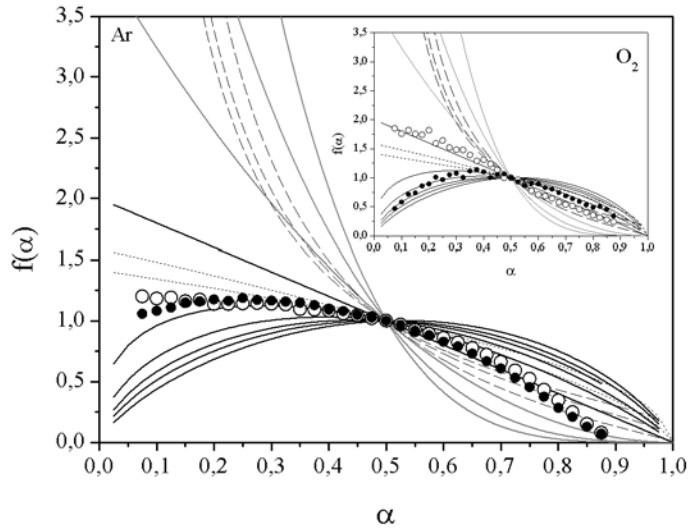
FIGURE 7
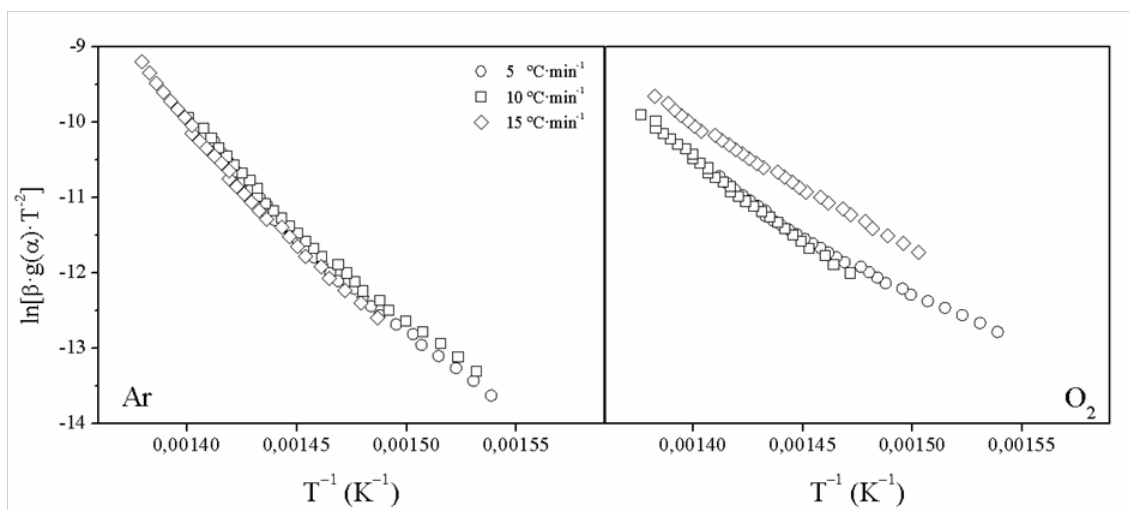
Table 1. Percentage of mass-loss for virgin PET and its recyclates after thermal and thermo-oxidative decomposition.

VPET		RPET-1		RPET-2		RPET-3		RPET-4		RPET-5	
Mass loss	e	Mass loss	e	Mass loss	e	Mass loss	e	Mass loss	e	Mass loss	e
79,9	1,2	81,2	3,1	81,7	2,2	83,4	3,6	84,2	2,5	84,8	2,5
78,5	3,1	77,3	2,5	77,9	3,3	78,7	4,2	78,2	3,6	79,9	4,1
21,1	2,1	22	2,8	21,4	2,7	21	3,9	21,1	3,1	20	3,3

*Average and errors taken from the analyses at different heating rates. Values given in percentages.

30

Table 2. Summary of main evolved gases during thermal and thermo-oxidative decompositions, as analysed by FT-I

Compound	Wavenumber (cm^{-1})	Vibrations *	Relative intensity in FTIR spectra	
			Ar	O$_2$
Acetaldehyde	2968	υ (CH$_3$)	↑↑	↑↑
	2740	υ (CHO)		
	1762	υ (C=O)		
	1414+1371	δ (CH$_3$)		
	1127	υ (C-O)		
Benzaldehyde	2690	υ (CHO)	↑	↓
	1724	υ (C=O)		
	1081	υ (C-O)		
	936	δ_{oop} (C-H)$_{arom}$		
CO$_2$	2356	υ_{as} (O=C=O)	↑↑	↑↑
CO	2174 + 2116	υ (C≡O)	↑↑	↓
* Notation on vibrations				
υ: stretching / δ: in-plane bending / as: asymmetric /oop: out-of-plane				

Figure 6.FT-IR spectra at the maximum decomposition rates of the thermo-oxidative decompositions of virgin PET. Tp1 and Tp2 stand for the first and second mass-loss peaks, respectively

31

Table 3.Ranges of n for A_n kinetic model for thermal and thermo-oxidative decomposition.

		VPET		RPET-1		RPET-2		RPET-3		RPET-4		RPET-5	
	method	n	$e_{P\text{-}Mc}$	n	$e_{P\text{-}Mc}$	n	$e_{P\text{-}Mc}$	n	$e_{P\text{-}Mc}$	n	$e_{P\text{-}Mc}$	n	$e_{P\text{-}Mc}$
Ar	$M\text{-}P_f$	1-1.5		1-1.5		1-1.5		1-1.5		1-1.5		1-1.5	
	$P\text{-}M_C$	1.380	1.45 %	1.365	1.52 %	1.223	1.11 %	1.384	1.12 %	1.371	1.31 %	1.375	1.21 %
O$_2$	$M\text{-}P_f$	1		1.5-2		1-1.5		2-2.5		2-2.5		1.5-2	
	$P\text{-}M_C$	1.012	3.18 %	1.892	3.52 %	1.642	4.13 %	2.368	5.22 %	2.151	4.01 %	1.710	3.62 %

Table 4.average values of activation energies obtained by Flynn-Wall-Ozawa (FWO), Kissinger-Akahira-Sunose (KAS) and calculation of average energy for further analysis, at both testing environments.

		Ea_{FWO}		Ea_{KAS}		Ea_{VYZ}		Ea_{iso}	
Conditions	Material	$(kJ \cdot mol^{-1})$	e_{FWO}	$(kJ \cdot mol^{-1})$	e_{KAS}	$(kJ \cdot mol^{-1})$	e_{VYZ}	$(kJ \cdot mol^{-1})$	e_{iso}
Ar	VPET	194	3,1 %	193	3,6 %	191	3,3 %	192	3,3 %
	RPET-1	198	3,0 %	197	3,1 %	198	2,1 %	197	2,7 %
	RPET-2	210	3,2 %	212	3,7 %	211	2,8 %	221	3,2 %
	RPET-3	188	5,3 %	187	5,4 %	187	4,1 %	187	4,9 %
	RPET-4	186	5,0 %	184	5,1 %	185	4,2 %	185	4,7 %
	RPET-5	190	4,2 %	191	3,0 %	190	3,6 %	190	3,6 %
O₂	VPET	196	20,3 %	195	22,0 %	192	17,3 %	194	19,8 %
	RPET-1	139	26,6 %	141	27,1 %	136	22,6 %	138	25,4 %
	RPET-2	140	23,6 %	141	22,2 %	137	20,4 %	139	22,1 %
	RPET-3	120	28,9 %	122	27,3 %	117	25,3 %	119	27,2 %
	RPET-4	115	22,9 %	118	23,2 %	113	19,8 %	115	21,9 %
	RPET-5	124	25,1 %	128	27,2 %	124	23,2 %	125	25,2 %

33

Badia, J. D., Martinez-Felipe, A., Santonja-Blasco, L., Ribes-Greus, A. (2013). Thermal and thermo-oxidative stability of reprocessed poly (ethylene terephthalate). *Journal of analytical and applied pyrolysis*, *99*, 191-202.

Table 5.Simplified kinetic triplets (SKT) for virgin PET and its recyclates under thermal and thermo-oxidative d

	Material	Ea_{P-Mc} (kJ·mol^{-1})	$e_{Ea\ P-Mc}$	Model A_n n_{P-Mc}	lnA_{P-Mc} (s^{-1})	$e_{\ lnAP-Mc}$
Ar	VPET	192	1.8 %	1,372	27,22	1,8 %
	RPET-1	197	1,6 %	1,375	28,13	1,8 %
	RPET-2	221	0,6 %	1,171	32,26	0,8 %
	RPET-3	187	1,4 %	1,384	26,32	1.6 %
	RPET-4	185	2,4 %	1,366	25,92	2,8 %
	RPET-5	190	1,3 %	1,359	26,89	1,5 %
O$_2$	VPET	194	7,4 %	0,657	28,36	7,8 %
	RPET-1	138	16,3 %	1,038	18,15	18,3 %
	RPET-2	139	13,4 %	1,043	18,54	14,4 %
	RPET-3	119	21,6 %	1,011	14,87	25,1 %
	RPET-4	115	7,1 %	1,190	13,90	8,7 %
	RPET-5	125	11,1 %	0,960	15,76	13,5 %